

## ENC-2022-0380

# DISTRIBUTED MATHEMATICAL MODEL AND EXPERIMENTAL VALIDATION FOR A CO<sub>2</sub> HEAT PUMP ASSISTED BY SOLAR ENERGY

### Humberto de Oliveira Reis

Federal University of Minas Gerais (UFMG), Post-Graduate Program in Mechanical Engineering, Av. Antonio Carlos, 6627, Belo Horizonte (MG), 31270-901, Brazil and  
humbertooreis@gmail.com

### Tiago de Freitas Paulino

Federal Center of Technological Education of Minas Gerais (CEFET-MG), Department of Materials Engineering, Av. Amazonas, 5253, Nova Suíça, 30421-169, Belo Horizonte (MG), Brazil  
tfpaulinoeng@gmail.com

### Luiz Machado

### Willian Moreira Duarte

Federal University of Minas Gerais (UFMG), Department of Mechanical Engineering, Av. Antonio Carlos, 6627, Belo Horizonte - MG, 31270-901, Brazil  
luizm@demec.ufmg.br, willianmoreira@ufmg.br

**Abstract.** A use of CO<sub>2</sub> operating in a transcritical cycle has been proven for heat pumps is a demonstrably viable and considerably interesting option due to the environmental advantages of CO<sub>2</sub> over other refrigerant gases. In order to improve the energy performance of systems that use heat pumps, integrating a type of energy such as renewable geothermal, solar, wind and bio-fuels must be available. In this scenario, a mathematical model with experimental validation of the components that allows the modeling of the heat pump system to vary the input parameters and determine the outlet water temperature and the coefficient of performance (COP) of the heat pump. This article approaches the modeling of the DX-SAHP, in order to obtain the profile of temperature and pressure distribution along the gas cooler, and the values of heat exchange and pressure in collector solar/evaporator. The model was validated with experimental data from 88 tests performed under different operating conditions, even the DX-SAHP in question. In the experimental the radiation incidence range in the study environment was from 0 to 845 W/m<sup>2</sup> and at an ambient temperature of 21°C to 33°C. The maximum difference between the theoretical results and experimental results was 9.5%.

**Keywords:** DX-SAHP, Mathematical Mode, Evaporator

## 1. INTRODUCTION

Faced with the gradual increase in temperature over time, global warming is an important problem to consider to make the global economy sustainable. In this scenario, researchers looking for ways to reduce greenhouse gas emissions and maximize equipment performance. In the refrigeration area the Carbon dioxide (CO<sub>2</sub> or R744) as a refrigerant fluid has zero net impact in climate change and it is a not toxic, corrosive fluid or flammable, it is inexpensive and readily available fluid.

The refrigerant fluid, in addition, technical solutions with better energy efficiency are used, for example for heating water, heat pumps show a COP (Coefficient of Performance) between 2 and 3, even more allied with the use of solar energy to maximize efficiency. In this case, this type of equipment is called Solar Assisted Heat Pump (SAHP).

The table 1, list different articles to study heat pump. to different types of collators UFP (Uncovered Flat Plate) CFP (Covered Flat Plat) PVT (PhotoVoltaic Thermal). Only two articles of the table 1 use Heat Pumps with R744. The mathematical model presented by Duarte *et al.* (2019a) was validated using R134a although excellent values of relative errors the R744 is not used to experimental validation. Diniz *et al.* (2021) the model is complex, transient, and demand very cost computational and the experimental validation was made qualitatively, to exemplify the COP, which is one of the most important variables from the energy point of view of a heat pump, there is no experimental validation, in the study, only an analysis of the response is performed as a function of the variation in the area of the expansion device.

Authors	Collector Type	Collector size (m <sup>2</sup> )	Refrigerant	Experimental Validation	Relative error (%)	Location	Tank size (L)	Water Temp. (°C)
Chaturvedi and Shen (1984)	UFP	3.4	R12	✓	-	Norfolk	-	-
Chaturvedi <i>et al.</i> (1998)	UFP	3.5	R12	✓	-	Norfolk	-	-
Ito <i>et al.</i> (1999)	UFP	3.2	R22	✓	-	Japan	-	30-60
Torres-Reyes and Gortari (2001)	UFP	4.5	R22	✓	-	Guanajuato	-	-
Hawladar <i>et al.</i> (2001)	UFP	3.0	R134a	✓	-	Singapore	250	55
Chyng <i>et al.</i> (2003)	UFP	1.9	R134a	✓	10 (max.)	Taiwan	-	52-56
Kuang <i>et al.</i> (2003)	UFP	2.0	R22	✓	5-30	Shanghai	150	50
Chata <i>et al.</i> (2005)	UFP	-	R404A, R407C, R410A R12, R22 and R134a	✗	N.A.	-	-	-
Xu <i>et al.</i> (2009)	PVT	2.3	R22	✗	N.A.	Nanjing	150	50
Chow <i>et al.</i> (2010)	UFP	12	R134a	✗	N.A.	Hong Kong	1500	50
Kong <i>et al.</i> (2011)	UFP	4.2	R22	✓	1-4.6	Shanghai	150	50
Moreno-Rodríguez <i>et al.</i> (2012)	UFP	5.6	R134a	✓	10 (max.)	Madrid	300	51
Chaturvedi <i>et al.</i> (2014)	UFP	1-5	R134a	✗	N.A.	Norfolk	-	50-70
Sun <i>et al.</i> (2015)	UFP	2.0	-	✗	N.A.	Shanghai	150	55
Deng and Yu (2016)	CFP	2.5	R134a	✗	N.A.	-	150	55
Kong <i>et al.</i> (2017)	UFP	4.2	R410A	✗	N.A.	-	150	50
Mohamed <i>et al.</i> (2017)	UFP	4.2	R407C	✓	4 (max.)	Nottingham	200	50
Duarte <i>et al.</i> (2019a)	UFP	1.6	R134a, R600a, R290, R1234yf and R744	✓	≅5 (max.) 1.6 (mean)	Belo Horizonte	200	65
Rabelo <i>et al.</i> (2019)	UFP	1.3-6	R134a and R290	✓	-	Belo Horizonte	200	65
Kong <i>et al.</i> (2020)	UFP	2.1	R134a	✓	10 (max.)	-	200	60
Diniz <i>et al.</i> (2021)	UFP	1.6	R744	✓	-	Belo Horizonte	200	≅40
Wang <i>et al.</i> (2021)	UFP	2.1	R134a	✓	-	-	200	30-50
Ma <i>et al.</i> (2021)	UFP	≅ 2.3	R22	✓	13 (max.)	-	-	-

Table 1. Studies with complete mathematical models for DX-SAHP

The purpose of this study is present and validate a mathematical model to steady state with low computational cost with relative error estimated at 10 %.

## 2. MATHEMATICAL MODEL

To evaluate the performance of DX-SAHP for the production of hot water, a steady-state model was developed using the Equation Engineering Solver (EES) similar to the model described by Duarte *et al.* (2018). Losses in the pipes connecting the components were considered negligible. The evaporator/solar collector and gas cooler were assumed to be isobaric. A lumped model was used for the evaporator and a distributed model was used for the gas cooler.

For validation of the mathematical model, the data published by Duarte *et al.* (2021) was used, which has a total of 88 experiments. The model needs as input data the relative humidity, and for that, only 41 experiments had the information, thus, the validation was performed with these 41 experiments. To obtain the 10 coefficients of the compressor's electrical power equation AHRI (2020), a multiple linear regression was performed as described by Chapra and Canale (2008), using 37 experimental points not contained in the set of experiments used to validate the model and the other 10 experiments remaining in the article were not used.

### 2.1 Compressor model

The hermetic compressor selected for this work is the model: SRcADB 6455, manufactured by SANDEN. In the literature, compressor models are described in detail (Yang *et al.*, 2013; Duarte *et al.*, 2019b; Bell *et al.*, 2020), but these models require many parameters and geometric details that are not provided by hermetic compressor manufacturers. Moreover, the compressor model used that integrates the complete model of the refrigeration system is simpler, assuming an isentropic compression process, as used in other studies (Minetto, 2011; Rabelo *et al.*, 2019; de Paula *et al.*, 2020). The compressor manufacturer does not provide the coefficients for AHRI (2020) equation to evaluate the electrical power

consumed by the compressor ( $\dot{W}_{cp}$ ). These coefficients were found by linear regression using 37 experiments. The equation are a function of evaporator pressure ( $P_e$ ) and gas cooler pressure ( $P_c$ ):

$$\dot{W}_m = C_1 + C_2P_e + C_3P_c + C_4P_e^2 + C_5(P_eP_c) + C_6P_c^2 + C_7P_e^3 + C_8(P_e^2P_c) + C_9(P_eP_c^2) + C_{10}P_c^3 \quad (1)$$

Table 2. Coeficients of electrical power consumed by the compressor.

Coefficient	Value
C1	-3,049114E+04
C2	3,088764E+01
C3	1,115466E+03
C4	6,674906E+00
C5	-7,292516E+00
C6	-1,184790E+01
C7	-1,346469E+01
C8	-6,224440E-0,2
C9	7,600259E-02
C10	3,608758E-02

The refrigerant mass flow rate ( $\dot{m}_r$ ) for a constant rotation speed reciprocating compressor is given by (Minetto, 2011):

$$\dot{m}_r = \rho_1 N V_s \eta_v \quad (2)$$

where  $\rho$  is the refrigerant density,  $N$  is the rotation speed,  $V_s$  is the compressor swept volume,  $\eta_v$  is the volumetric efficiency and the subscript 1 refers to compressor inlet or evaporator outlet.

The volumetric efficiency was determined by fitting equations proposed by Duarte *et al.* (2019a) to the compressor performance map provided by the manufacture. The volumetric and overall efficiencies is given by:

$$\eta_v = -0.0922 \left( \frac{P_c}{P_e} \right) + 0.9496 \quad (3)$$

## 2.2 Direct expansion solar evaporator model

The heat transfer rate received by the refrigerant in the evaporator ( $\dot{Q}_{rev}$ ) is given by:

$$\dot{Q}_{rev} = \dot{m}_r (i_1 - i_4) \quad (4)$$

where the subscript 4 refers to thermostatic valve outlet or evaporator inlet. To evaluate the energy gain from air and solar radiation in a flat plate collector in steady-state condition, Kong *et al.* (2011) suggest the following equation:

$$\dot{Q}_{air} = A_e F' [aI - U_L (\bar{T}_r - T_a)] \quad (5)$$

where  $A_e$  is the area of solar evaporator,  $F'$  is the collector effectiveness factor,  $I$  is the solar radiation,  $a$  is the solar absorptivity,  $U_L$  is overall heat loss coefficient,  $\bar{T}_r$  is the average temperature of the refrigerant fluid and  $T_a$  is the ambient air temperature.

The collector effectiveness factor proposed by Duffie and Beckman (2013), considering that the resistance to heat flow due the bond between the collector plate and tube can be neglected, is given by:

$$F' = \frac{1}{w U_{ev}} \left\{ \frac{1}{U_L [D_o + F(w - D_o)]} + \frac{1}{\pi D_i h_i} \right\}^{-1} \quad (6)$$

where the distance between the tubes in the evaporator is  $w$ , the fin efficiency is  $F$ , the outer diameter is  $D_o$ , the inner diameter is  $D_i$ , the internal convective coefficient is  $h_i$ , that is calculated by the correlation proposed by Shah (2017) for two phase flow, and by the correlation proposed by Gnielinski (1976), for single phase flow. Shah (2017) presented a new correlation and compared the results with another seven correlations, using 4852 experimental data points from 81 sources and 30 different fluids including R744.

The fin efficiency can be evaluated by:

$$F = \frac{\tanh \left[ (w - D_o) / 2 \sqrt{U_L / (k\delta)} \right]}{(w - D_o) / 2 \sqrt{U_L / (k\delta)}} \quad (7)$$

where  $\delta$  is the fin thickness and  $k$  is the thermal conductivity.

The overall heat loss coefficient proposed by Duffie and Beckman (2013) is determined by:

$$U_L = (h_{conv} + h_{cond} + h_{rad})_{bot} + (h_{conv} + h_{cond} + h_{rad})_{top} \quad (8)$$

where the subscripts *bot* and *top* represents the values at the bottom and top surface of the collector respectively. The convective coefficient ( $h_{conv}$ ) is calculated by the correlation proposed by Kumar and Mullick (2010), the condensation convective coefficient ( $h_{cond}$ ) from humid air is determined by the correlation proposed by Scarpa and Tagliafico (2016), the radiation heat transfer coefficient ( $h_{rad}$ ) is given by:

$$h_{rad} = \varepsilon\sigma(\bar{T}_r + T_a)(\bar{T}_r^2 + T_a^2) \quad (9)$$

where the emissivity is  $\varepsilon$ , and the Stefan-Boltzmann constant is  $\sigma$ .

### 2.3 Gas cooler model

In the gas cooler model the following assumptions were made: (i) the thermal losses to environment and pressure drop are negligible; (ii) the properties of the walls, CO<sub>2</sub> and H<sub>2</sub>O are equally distributed in the gas cooler section; (iii) thermal resistance of the wall tube due conduction is zero; and (iv) CO<sub>2</sub> and H<sub>2</sub>O flow is one-dimensional. The energy balance for carbon dioxide, tube wall and water in any section of the gas cooler showed in Fig. 1, is given by:

$$\dot{m}_r \frac{\partial i_r}{\partial z} = h_r p_{ii} (T_s - T_r) \quad (10)$$

$$h_r p_{ii} (T_s - T_r) = h_w p_{oi} (T_w - T_s) \quad (11)$$

$$h_w p_{oi} (T_w - T_s) = -\dot{m}_w \frac{\partial i_w}{\partial z} \quad (12)$$

where  $p$  is the perimeter,  $z$  is the gas cooler position. Subscripts  $r$ ,  $s$  and  $w$  refers to carbon dioxide, tube wall and water properties. Variables with subscripts  $ii$ ,  $io$  and  $oi$  are geometrical parameter calculated with the diameters showed in Fig. 1. The convective coefficient  $h$  is calculated by the correlation proposed by Gnielinski (1976) for both, fluids and correct by Gosse (1981) factor for flow in annular region.

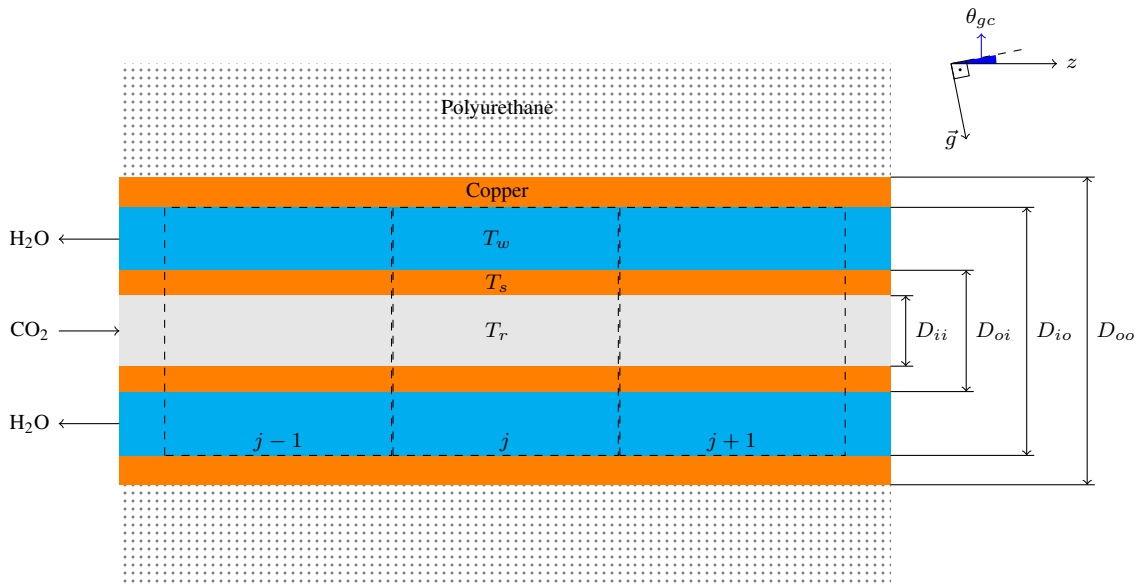


Figure 1. Gas cooler section geometry and control volume numbering

The boundary condition are the inlet temperature of water and refrigerant. To solve this system of differential equations, the finite volume technique and the central difference scheme described by Versteeg and Malalasekera (2007) were used. This system of differential equations becomes the system of algebraic equations given by:

$$\dot{m}_r \frac{i_r(j) - i_r(j-1)}{\Delta z} = h_r p_{ii} [T_s(j) - T_r(j)] \quad (13)$$

$$T_r(j) = \frac{h_w p_{oi} T_w(j) + h_r p_{ii} T_r(j)}{h_w p_{oi} + h_r p_{ii}} \quad (14)$$

$$h_w p_{oi} [T_w(j) - T_s(j)] = -\dot{m}_w \frac{i_w(j) - i_w(j+1)}{\Delta z} \quad (15)$$

The enthalpy variables represent values at the outlet edge and the temperatures variable represent the values at the center of control volume. The simultaneous solution of the nonlinear system of equations would result in huge arrays with difficult convergence. An iterative solution is described by Machado (1996) that allow solve the equations for refrigerant and water separately. This iterative solutions is described in Fig. 2, where  $E_{tol}$  is a tolerance error,  $E_{Tr}$  is the refrigerant temperature convergence error and  $E_{Ts}$  is the wall temperature convergence error. This errors are given by:

$$E_{Tr} = \frac{T_r^p - T_r}{T_r} \cdot 100 \quad (16)$$

$$E_{Ts} = \frac{1}{n} \sum_{j=1}^n \frac{T_s^p(j) - T_s(j)}{T_s(j)} \cdot 100 \quad (17)$$

where the superscript  $p$  represents the value at previous iteration and  $n$  is the number of control volumes.

### 3. RESULTS AND DISCUSSION

#### 3.1 Grid test

A spatial grid test was performed to determine the size of the control volumes in the gas cooler ( $\Delta z$ ), following the directives described McHale and Friedman (2009). In this simulation was done considering the gas cooler pressure of 80 bar, ambient and inlet water temperature of 25°C, no wind, a solar radiation of 500 W/m<sup>2</sup> and a water flow rate of 28.8 L/h. For control volumes smaller than 110.5 mm, the changes in the values of  $COP$  and  $T_{wo}$  were smaller than the convergence tolerance error. Table 3 shows the results of the simulation done in the grid test.

Table 3. Results of grid test for 80 bar, 25°C, 0 m/s, 500 W/m<sup>2</sup> and 28.8 L/h

$\Delta z$ (mm)	$COP$	$\Delta COP$ (%)	$T_{wo}$ (°C)	$\Delta T_{wo}$ (%)
243	2.4198		63.258	
186.9	2.4790	-2,4	64.209	-1.5
143.8	2.5067	-1.1	64.712	-0.8
110.5	2.5217	-0.6	64.997	-0.4
85	2.5349	-0.5	65.246	-0.4

Then, after the spatial grid test, the following results were based in the list of parameters presented in Tab. 4. The carbon dioxide, water, air and copper properties were calculated using internal EES libraries.

Table 4. Simulations parameters list

Parameter	Value	Parameter	Value
Atmospheric Pressure	905.0 kPa	Wind Speed	0 m/s
Emissivity	0.95	Solar absorptivity	0.95
Compressor displacement	1.75 cm <sup>3</sup> /rev	Compressor rotation speed	3500 rpm
Ambient temperature	25 °C	$E_{tol}$	±0.5 %
$\Delta z$	110.5 mm	Collector length	1563.4 mm
Collector width	1000.4 mm	Collector fin thickness	0.55 mm
Collector tube lenght	16.3 mm	Collector tube inner diameter	4.66 mm
Collector tube outer diameter	6.34 mm	Collector distance between the tubes	92.5 mm
Gas cooler tube lenght	24.3	Gas cooler tube outer dia. (flow Water)	12.5 mm
Gas cooler tube inner diameter (flow CO2)	4.66 mm	Gas cooler tube inner dia. (flow Water)	10.52 mm
Gas cooler tube outer diameter (flow CO2)	6.34 mm		

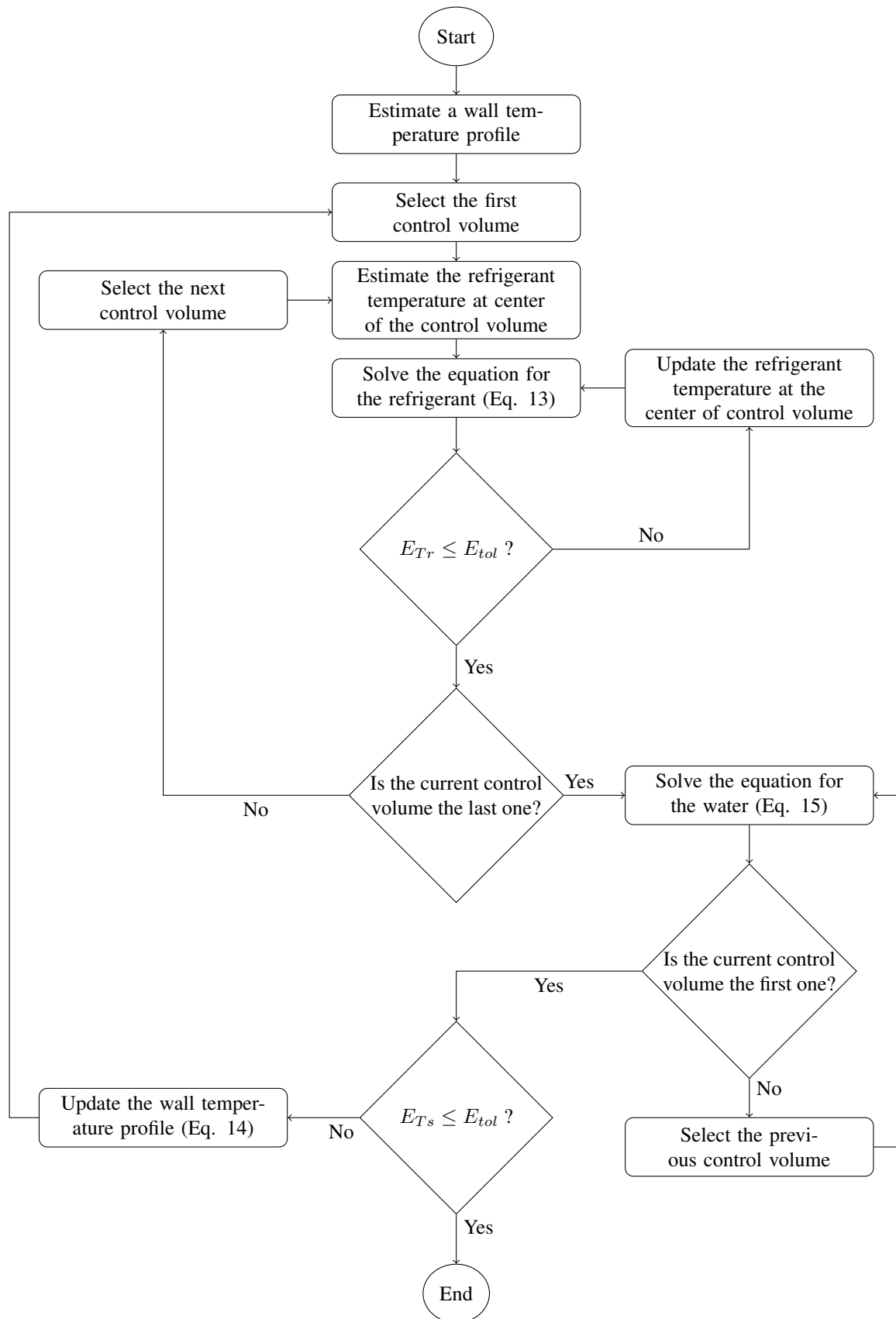


Figure 2. Flow chart for solving the gas cooler equations



Figure 3. Correlation between measured COP x theoretical COP

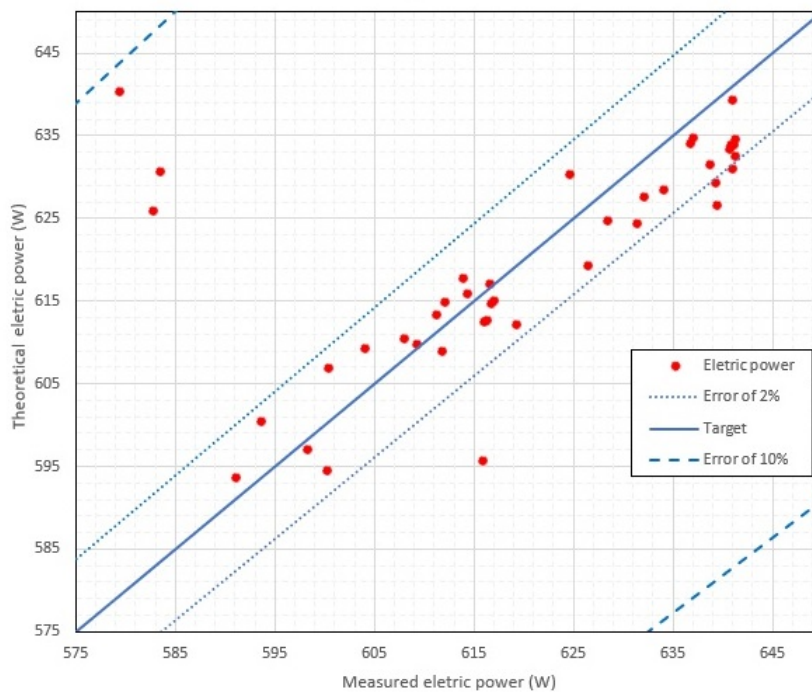


Figure 4. Correlation between measured electric power x theoretical electric power

### 3.2 Validation

The COP correlation graphics shows the distribution of the measured COP versus simulated and the distribution of points puts only 3 points out of 41 with the error above 5 %. The maximum error observed was 8.4%, and the mean absolute error was 2.7%. The simulation of the electrical power consumed by the compressor compared to the measurement also showed a satisfactory adjustment as observed in the graph, only 5 points out of 41 have an error above

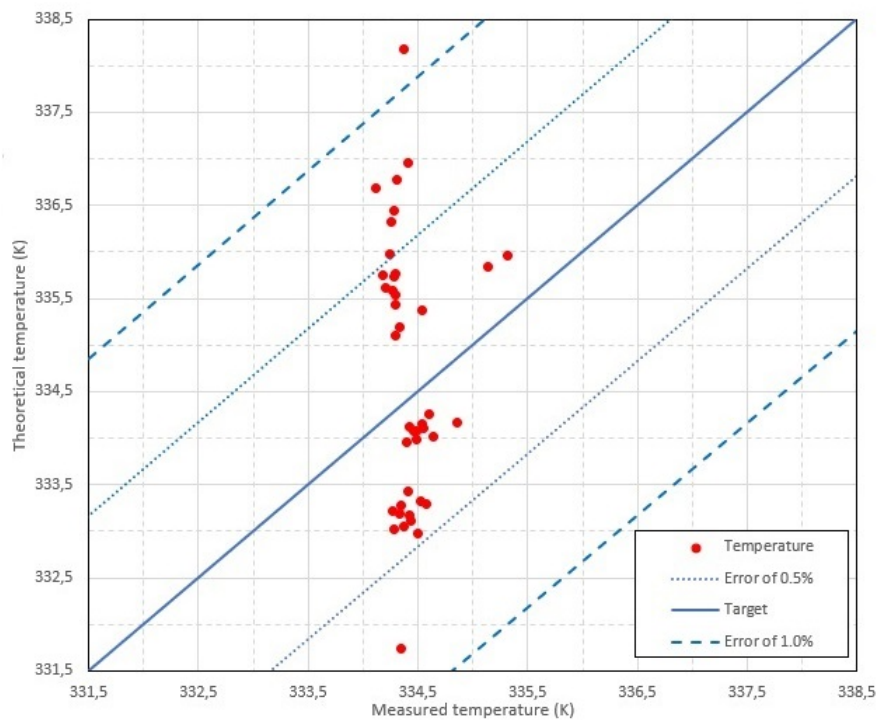


Figure 5. Correlation between outlet water temperature x theoretical temperature

2%. The maximum error observed is 9.5% and the mean absolute error was 1.36%. The temperature graph shows that the errors are within a maximum error of 1.1%.

According to table 1, the maximum observed errors observed in the mathematical models presented are similar to the values found in several articles.

#### 4. CONCLUSION

In this study, a set of experimental data from a CO<sub>2</sub> Heat Pump Assisted by Solar Energy published by Duarte *et al.* (2021), was used to validate the mathematical model. To concentric counter flow gas cooler was used a distributed model, and to the components: evaporator, compressor and expansion valve was used a lumped model.

In the results analysis, the present mathematical model proved to be efficient to predict the COP and the outlet water temperature, and the maximum error less than 10% is in agreement with other models predicted in the literature. Its useful only steady state regime and simulations and has low computational cost for simulation.

#### 5. REFERENCES

- AHRI, 2020. *CAN/ANSI/AHRI 540-2020, Performance Rating of Positive Displacement Refrigerant Compressors*. Air Conditioning, Heating and Refrigeration Institute.
- Bell, I.H., Ziviani, D., Lemort, V., Bradshaw, C.R., Mathison, M., Horton, W.T., Braun, J.E. and Groll, E.A., 2020. “Pdsim: A general quasi-steady modeling approach for positive displacement compressors and expanders”. *International Journal of Refrigeration*, Vol. 110, pp. 310–322.
- Chapra, S.C. and Canale, R.P., 2008. *Métodos numéricos para engenharia*. McGraw-Hill.
- Chata, F.G., Chaturvedi, S. and Almogbel, A., 2005. “Analysis of a direct expansion solar assisted heat pump using different refrigerants”. *Energy Conversion and Management*, Vol. 46, No. 15, pp. 2614–2624.
- Chaturvedi, S., Chen, D. and Kheireddine, A., 1998. “Thermal performance of a variable capacity direct expansion solar-assisted heat pump”. *Energy Conversion and management*, Vol. 39, No. 3, pp. 181–191.
- Chaturvedi, S., Gagrani, V. and Abdel-Salam, T., 2014. “Solar-assisted heat pump – a sustainable system for low-temperature water heating applications”. *Energy Conversion and Management*, Vol. 77, pp. 550 – 557.
- Chaturvedi, S.K. and Shen, J.Y., 1984. “Thermal performance of a direct expansion solar-assisted heat pump”. *Solar Energy*, Vol. 33, No. 2, pp. 155 – 162.
- Chow, T.T., Pei, G., Fong, K., Lin, Z., Chan, A. and He, M., 2010. “Modeling and application of direct-expansion solar-assisted heat pump for water heating in subtropical hong kong”. *Applied Energy*, Vol. 87, No. 2, pp. 643–649.



- Chyng, J., Lee, C. and Huang, B., 2003. “Performance analysis of a solar-assisted heat pump water heater”. *Solar Energy*, Vol. 74, No. 1, pp. 33 – 44.
- de Paula, C.H., Duarte, W.M., Rocha, T.T.M., de Oliveira, R.N., de Paoli Mendes, R. and Maia, A.A.T., 2020. “Thermo-economic and environmental analysis of a small capacity vapor compression refrigeration system using R290, R1234yf, and R600a”. *International Journal of Refrigeration*, Vol. 118, pp. 250–260.
- Deng, W. and Yu, J., 2016. “Simulation analysis on dynamic performance of a combined solar/air dual source heat pump water heater”. *Energy Conversion and Management*, Vol. 120, pp. 378 – 387.
- Diniz, H.A.G., Paulino, T.F., Pabon, J.J.G., Maia, A.A.T. and Oliveira, R.N., 2021. “Dynamic model of a transcritical CO<sub>2</sub> heat pump for residential water heating”. *Sustainability*, Vol. 13, No. 6.
- Duarte, W.M., Paulino, T.F., Rabelo, S.N., Machado, L. and Maia, A.A.T., 2018. “Optimal high pressure correlation for R744 direct expansion solar assisted heat pump for domestic hot water”. In *17th Brazilian Congress of Thermal Sciences and Engineering (to appear)*. ABCM.
- Duarte, W.M., Paulino, T.F., Pabon, J.J., Sawalha, S. and Machado, L., 2019a. “Refrigerants selection for a direct expansion solar assisted heat pump for domestic hot water”. *Solar Energy*, Vol. 184, pp. 527 – 538. ISSN 0038-092X.
- Duarte, W.M., Rabelo, S.N., Paulino, T.F., Pabón, J.J. and Machado, L., 2021. “Experimental performance analysis of a CO<sub>2</sub> direct-expansion solar assisted heat pump water heater”. *International Journal of Refrigeration*, Vol. 125, pp. 52–63.
- Duarte, W.M., Pabon, J.J.G., Maia, A.A.T. and Machado, L., 2019b. “Nonisentropic phenomenological model of a reciprocating compressor”. *International Journal of Air-Conditioning and Refrigeration*, p. 1950039.
- Duffie, J.A. and Beckman, W.A., 2013. *Solar engineering of thermal processes*. John Wiley & Sons.
- Gnielinski, V., 1976. “New equations for heat and mass transfer in turbulent pipe and channel flow”. *Int. Chem. Eng.*, Vol. 16, No. 2, pp. 359–368.
- Gosse, J., 1981. *Guide technique de thermique*. Dunod.
- Hawladar, M., Chou, S. and Ullah, M., 2001. “The performance of a solar assisted heat pump water heating system”. *Applied Thermal Engineering*, Vol. 21, No. 10, pp. 1049 – 1065.
- Ito, S., Miura, N. and Wang, K., 1999. “Performance of a heat pump using direct expansion solar collectors”. *Solar Energy*, Vol. 65, pp. 189–196.
- Kong, X., Wang, B., Shang, Y., Li, J. and Li, Y., 2020. “Influence of different regulation modes of compressor speed on the performance of direct-expansion solar-assisted heat pump water heater”. *Applied Thermal Engineering*, Vol. 169, p. 115007. ISSN 1359-4311.
- Kong, X., Li, Y., Lin, L. and Yang, Y., 2017. “Modeling evaluation of a direct-expansion solar-assisted heat pump water heater using R410a”. *International Journal of Refrigeration*, Vol. 76, pp. 136–146.
- Kong, X., Zhang, D., Li, Y. and Yang, Q., 2011. “Thermal performance analysis of a direct-expansion solar-assisted heat pump water heater”. *Energy*, Vol. 36, No. 12, pp. 6830–6838.
- Kuang, Y., Sumathy, K. and Wang, R., 2003. “Study on a direct-expansion solar-assisted heat pump water heating system”. *International Journal of Energy Research*, Vol. 27, No. 5, pp. 531–548.
- Kumar, S. and Mullick, S., 2010. “Wind heat transfer coefficient in solar collectors in outdoor conditions”. *Solar Energy*, Vol. 84, No. 6, pp. 956–963.
- Ma, K., Wang, Z., Li, X., Wu, P. and Li, S., 2021. “Structural optimization of collector/evaporator of direct-expansion solar/air-assisted heat pump”. *Alexandria Engineering Journal*, Vol. 60, No. 1, pp. 387–392. ISSN 1110-0168.
- Machado, L., 1996. *Modele de simulation et etude experimentale d'un evaporateur de machine frigorifique en regime transitoire*. Ph.D. thesis, INSA, Lyon.
- McHale, M. and Friedman, J., 2009. “Standard for verification and validation in computational fluid dynamics and heat transfer”. *The American Society of Mechanical Engineers, ASME V&V*, pp. 20–2009.
- Minetto, S., 2011. “Theoretical and experimental analysis of a CO<sub>2</sub> heat pump for domestic hot water”. *International journal of refrigeration*, Vol. 34, No. 3, pp. 742–751.
- Mohamed, E., Riffat, S. and Omer, S., 2017. “Low-temperature solar-plate-assisted heat pump: A developed design for domestic applications in cold climate”. *International Journal of Refrigeration*, Vol. 81, pp. 134 – 150.
- Moreno-Rodríguez, A., González-Gil, A., Izquierdo, M. and Garcia-Hernando, N., 2012. “Theoretical model and experimental validation of a direct-expansion solar assisted heat pump for domestic hot water applications”. *Energy*, Vol. 45, No. 1, pp. 704–715.
- Rabelo, S.N., Paulino, T.F., Machado, L. and Duarte, W.M., 2019. “Economic analysis and design optimization of a direct expansion solar assisted heat pump”. *Solar Energy*, Vol. 188, pp. 164 – 174. ISSN 0038-092X.
- Scarpa, F. and Tagliafico, L.A., 2016. “Exploitation of humid air latent heat by means of solar assisted heat pumps operating below the dew point”. *Applied Thermal Engineering*, Vol. 100, pp. 820 – 828.
- Shah, M.M., 2017. “Unified correlation for heat transfer during boiling in plain mini/micro and conventional channels”. *International Journal of Refrigeration*, Vol. 74, pp. 604–624.
- Sun, X., Dai, Y., Novakovic, V., Wu, J. and Wang, R., 2015. “Performance comparison of direct expansion solar-assisted

- heat pump and conventional air source heat pump for domestic hot water”. *Energy Procedia*, Vol. 70, pp. 394 – 401.
- Torres-Reyes, E. and Gortari, J.C., 2001. “Optimal performance of an irreversible solar-assisted heat pump”. *Exergy, An International Journal*, Vol. 1, No. 2, pp. 107 – 111.
- Versteeg, H.K. and Malalasekera, W., 2007. *An introduction to computational fluid dynamics: the finite volume method*. Pearson Education.
- Wang, B., Kong, X., Yan, X., Shang, Y. and Li, Y., 2021. “Influence of subcooling on performance of direct-expansion solar-assisted heat pump”. *International Journal of Refrigeration*, Vol. 122, pp. 201–209. ISSN 0140-7007.
- Xu, G., Deng, S., Zhang, X., Yang, L. and Zhang, Y., 2009. “Simulation of a photovoltaic/thermal heat pump system having a modified collector/evaporator”. *Solar Energy*, Vol. 83, No. 11, pp. 1967 – 1976.
- Yang, B., Bradshaw, C.R. and Groll, E.A., 2013. “Modeling of a semi-hermetic CO<sub>2</sub> reciprocating compressor including lubrication submodels for piston rings and bearings”. *International Journal of Refrigeration*, Vol. 36, No. 7, pp. 1925–1937. ISSN 0140-7007. *New Developments in Compressor Technology*.